

Analysis of Site Attenuation for Spherical Dipole Antenna and Its Application

Atsuto KITANI

Faculty of Engineering,
Kyushu Institute of Technology
1-1 Sensui-Cho, Tobata-ku, Kitakyushu-
Shi 804-8550, JAPAN
atsuto@buddy.elcs.kyutech.ac.jp

Nobuo KUWABARA

Faculty of Engineering,
Kyushu Institute of Technology
1-1 Sensui-Cho, Tobata-ku, Kitakyushu-
Shi 804-8550, JAPAN
kuwaba.nobuo@buddy.elcs.kyutech.ac.jp

Fujio AMEMIYA

NTT Advanced Technology,
Musashino-shi, Tokyo
180-8585 Japan
Amemiya@emc.ntt-at.co.jp

Abstract

Spherical dipole antenna has been used to evaluate EMC performance because it can consider small dipole source. In this paper, site attenuation of spherical dipole antenna is calculated using wire grid model. It is also measured in semi-anechoic chamber for 3m distance, and the result indicates the deviation between calculation and measurement result is within 4dB from 30 MHz to 1000MHz.

The site attenuation distribution is measured in a small semi-anechoic chamber and compared with the measured one.

The result indicates that the large reflection loss absorber is effective to improve the performance of the site and the site attenuation is improved when transmitting and receiving antenna place at line unsymmetrical position.

Keywords

Site Attenuation, Spherical Dipole Antenna Wire Grid NEC, Method of Moment

1. INTRODUCTION

Recent progress of EMC technology needs the antenna to eliminate the influence of the coaxial cable. The antenna with a transmitter and its battery [1] and the antenna replacing coaxial cable by optical fiber [2], [3] have been developed.

Spherical dipole antenna has been developed as a radiation source to evaluate EMC measurement facilities [1] and shielding effect of cabinets [4] because it can be considered an ideal small dipole source.

Site attenuation has widely used to evaluate EMI measurement facilities, and its characteristics have been studied for various antenna, such as half-wave dipole antenna [5] and biconical antenna [6]. However, the size of these antennas are too big to use of evaluating small measurement facilities such as small anechoic chamber. Study of the calculation method for spherical dipole antenna has been needed to develop EMI measurement technology.

This paper describes the calculation method of site attenuation for spherical dipole antenna. The transmitting and receiving antenna modeled wire grid and the site attenuation is calculated. The calculation results are compared

with measured one. The site attenuation distribution of small semi-anechoic chamber is evaluated to demonstrate its application.

2. ANALYSIS METHOD

2.1 Site attenuation analysis using method of moment

The site attenuation is the propagation loss between antennas placing on a site, and the Method of Moment (MoM) has been applied to analyze the site attenuation [5]. The calculation model is shown in Fig. 1. In Fig. 1, E and Z_t are the source of the transmitting antenna and $W_{t1} \dots W_{tn}$ are the wire elements of the transmitting antenna. I_r and Z_r are the received current and load of the receiving antenna respectively, and $W_{r1} \dots W_{rm}$ are the wire elements of receiving antenna.

On the calculation, A pair of antennas are modeled by wire element as shown in Fig. 1 and the relations between voltages and current are given by [7]

$$\begin{bmatrix} E \\ 0 \\ \vdots \\ 0 \end{bmatrix} = \begin{bmatrix} Z_{t1t1} + Z_t & \cdots & Z_{t1tm} & Z_{t1r1} & \cdots & Z_{t1rm} \\ \vdots & \ddots & \vdots & \vdots & \ddots & \vdots \\ Z_{mr1} & \cdots & Z_{mm} & Z_{mr1} & \cdots & Z_{mrn} \\ Z_{r1r1} & \cdots & Z_{r1m} & Z_{r1r1} & \cdots & Z_{r1m} \\ \vdots & \ddots & \vdots & \vdots & \ddots & \vdots \\ Z_{mr1} & \cdots & Z_{mm} & Z_{mr1} & \cdots & Z_{mrn} \end{bmatrix} \begin{bmatrix} I_{r1} \\ \vdots \\ I_m \\ I_{r1} \\ \vdots \\ I_m \end{bmatrix} \quad (1)$$

Where Z_{ii} is self-impedances and Z_{ij} is the mutual impedances between each element [7].

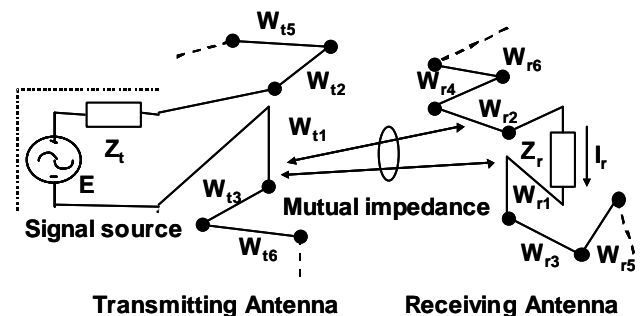


Fig. 1 Calculate model of Site Attenuation

The site attenuation, S_{ATT} , is defined by Eq. (2),

$$S_{ATT} (dB) = V_{through} - V_{site} = 20 \log_{10} \frac{E}{2Z_r I_{r1}} \quad (2)$$

Where $V_{through}$ is the output level in $dB\mu V$ when the cables to the transmitting and receiving antenna are connected directly, V_{site} is the output level in $dB\mu V$ when the cables are connected to the each antenna. Since we can obtain I_{r1} using the MOM, the site attenuation can be calculated from Eq. (1).

2.2 Wire grid model of spherical dipole antenna

The structure of spherical dipole antennas is shown in Fig. 2.

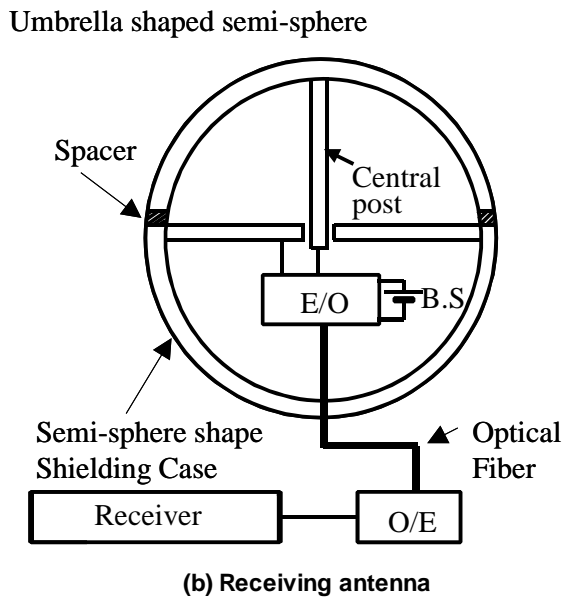
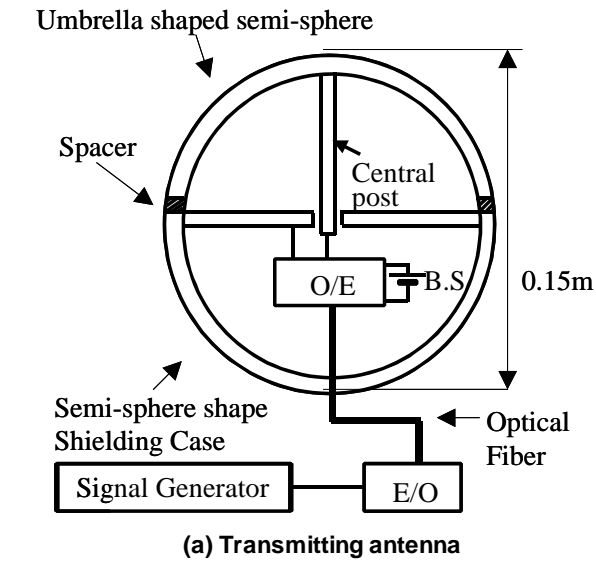


Fig. 2 Structure of transmitting and receiving spherical dipole antenna

The transmitting spherical dipole antenna is composed three parts that are spherical radiator, optical fiber, and electro-optical (E/O) converter. The radiator is divided into upper and lower part. The upper part is umbrella shaped semi-sphere to reduce capacitance between upper and lower part, and lower part is spherical shape shielding case where optical-electro (O/E) converter and battery supply (B.S.) is installed [2].

The receiving spherical dipole antenna has the same structure, where E/O and O/E converter in Fig. 2(a) are replaced by O/E and E/O converter respectively. The signal is supplied between upper and lower part of the transmitting antenna via optical fiber. The receiving signal appears between upper and lower part of receiving antenna and it is transmitted to the receiver via optical fiber. The diameters of these antennas are 0.15 m.

Wire grid model of spherical dipole antenna is shown in Fig. 3. A voltage source and an impedance, Z_t , are inserted between the central post and the shielding case for transmitting antenna, and an impedance, Z_r , is inserted between the central post and the shielding case for receiving antenna, where Z_t and Z_r is the internal impedance of O/E converter and the load impedance of E/O converter respectively.

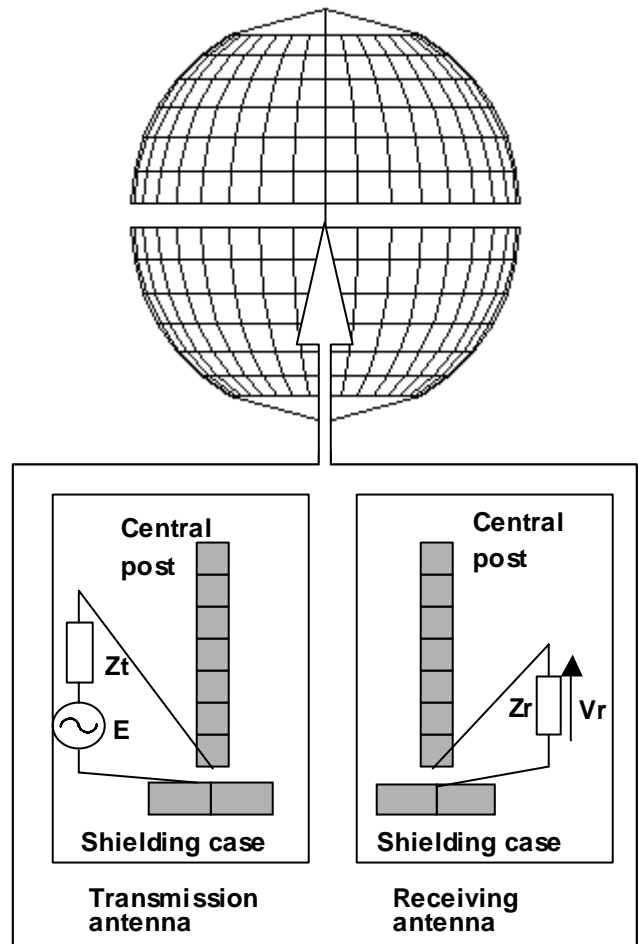


Fig.3 Wire grid model of spherical dipole antenna

The number of segment should be determined to calculate the sufficient convergent solution. The length of each wires are sufficiently short compared with wavelength in this analysis.

The number of the segment for the central post is important to get the converged solution because the large current flows on this post. The relations between the number of segment and the calculation result are investigated. Figure 4 show the deviation of the calculation result referred the measurement value at free space. This shows that the calculation value converged to the measurement value when the number of segment increased. When the number of segment is larger than 200, the solution diverges. Then, we select the segment number of 90 for calculation.

In addition, the antenna has a cylindrical symmetry. So, the wires are concentrated at the top and bottom area, and it may cause the calculation error. So, the number of wires should be controlled in these areas. Therefore, the relations between the numbers of wires and deviation of the calculation result in these areas are investigated.

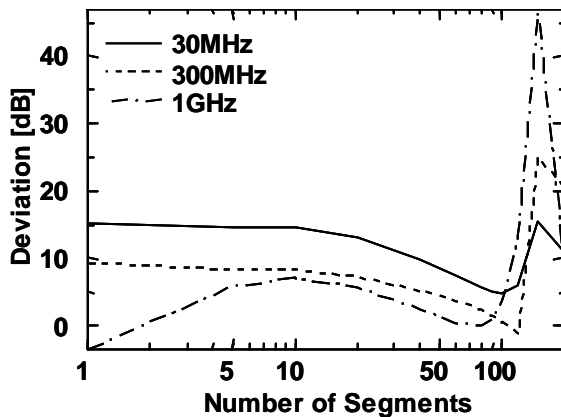


Fig. 4 Deviation of calculated site attenuation in free space.

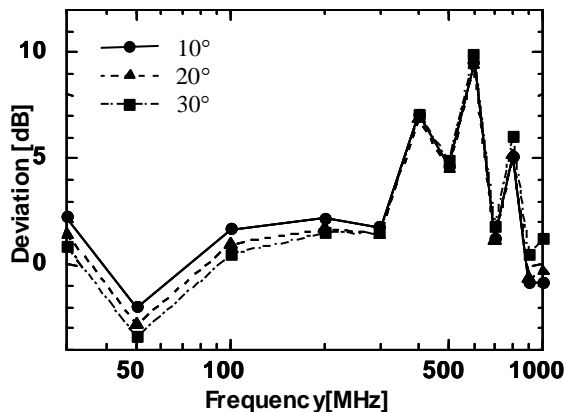


Fig. 5 Deviations of calculated site attenuation in free space by concentration of wires

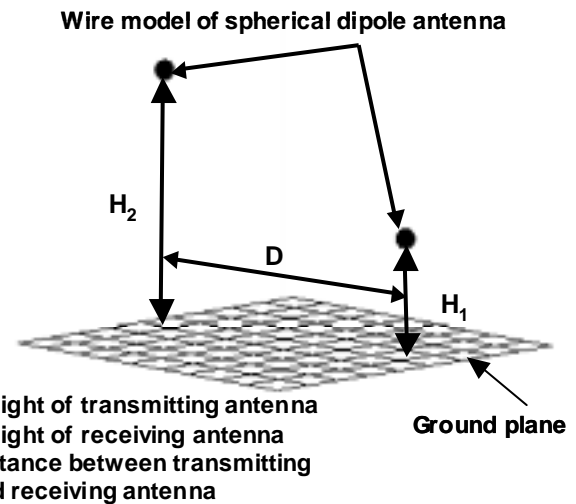
The number of wires is reduced to 4 in the area where the angle to the central post is 10, 20 and 30 degrees from the top and bottom of the model to reduce concentration of wires. Figure 5 shows the deviation of site attenuation between the calculation and the measurement value at free space. From this Figure, we select 30 degrees in less than 800MHz and 10 degrees in more than 800MHz for optimum value. When 30 degrees is selected, the model has 962 numbers of wires, 1001 number of segments. When 10 degrees is selected, the model has 1250 numbers of wires, 1428 number of segments. In addition, 3 mm diameters of wires are used for the outer area of the antenna. In this case, the calculation time is one and half times compared with the case of 30degrees.

2.3 Analysis of site attenuation

Figure 6 shows the layout of transmitting and receiving antenna to calculate the site attenuation. In this analysis, these antennas are placed on infinite and perfect conductivity ground plane. The wire grid positions are calculated based on the layout in Fig. 6. Numerical electromagnetic code (NEC)[8] is used to calculate the current I_r at Z_r . From Eq. (2), the site attenuation of spherical dipole is determined following equation.

$$S_{ATT} = 20 \log \frac{V_{in}}{V_{out}} = 20 \log \frac{2Z_0 L_r L_t}{(Z_t + Z_r)(Z_t + Z_r)} \frac{E}{I_{r1}} \quad (3)$$

Where V_{in} is the input voltage of E/O converter for transmission spherical dipole antenna, V_{out} is the output voltage of O/E converter for receiving spherical dipole antenna, Z_t is the output impedance of the O/E converter in the transmitting antenna, Z_r is the input impedance of the receiving antenna, L_r is transmission loss from E/O converter to O/E converter for receiving, and L_t transmission loss from E/O converter to O/E converter for transmitting antenna. L_r and L_t are measured using a network analyzer, and Z_0 is input impedance of the network analyzer.



H₁: Height of transmitting antenna
H₂: Height of receiving antenna
D: Distance between transmitting and receiving antenna

Fig. 6 Layout of transmitting and receiving antenna on ground plane

3. MEASUREMENT

3.1 Measurement set-up

The site attenuation was measured using measurement layout shown in Fig. 7. A semi-anechoic chamber, whose inner size was 29 m long, 15 m wide, and 9 m high, was used for measurement. The transmitting antenna was placed 1m high above ground plane, and the height of the receiving antenna changed from 1 m to 4 m. The horizontal distance between transmitting and receiving antenna was 3 m.

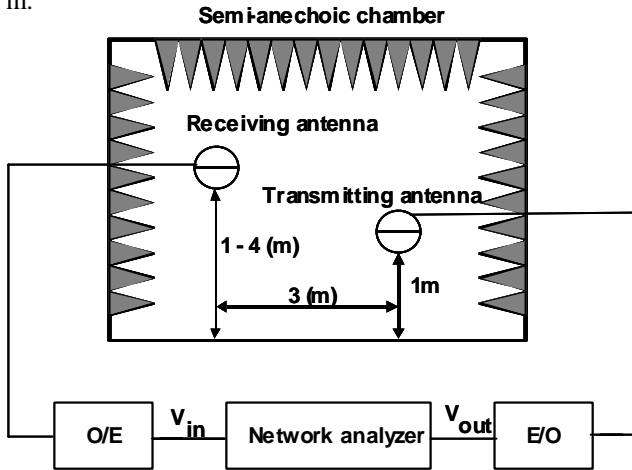


Fig. 7 Experimental set-up for measuring site attenuation

3.2 Measurement of site attenuation

The site attenuation defined by Eq. (3) was measured from 30 MHz to 1000 MHz by network analyzer. The measurement result is shown in Fig. 8. In this figure, vertical axis indicates the minimum value of the site attenuation. Dots indicate measured value, and solid line indicates calculation value. On the calculation, NEC-2 [8] software was used, and Z_t , Z_r , and Z_0 were 50 Ω . The attenuator of 6 dB was inserted between O/E converter and transmitting antenna element to stabilize the output impedance of the converter, and the attenuator of 10 dB is inserted between E/O converter and receiving antenna element for the same object. Figure 8 shows the measurement results almost agree with calculation value, whose deviation is within 4 dB from 30 MHz to 1000 MHz. These results mean that the calculation model in this paper is effective to calculate site attenuation of spherical dipole antenna.

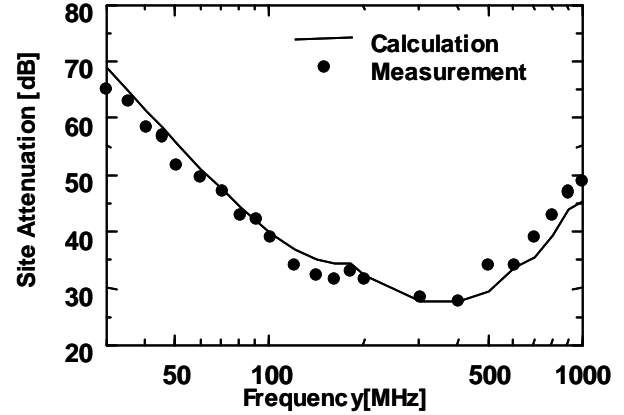
3.3 Measurement of antenna factor

Using calculation results of site attenuation, antenna factor was obtained and compared with measured one. The relation between site attenuation and antenna factor, F_a , is given by

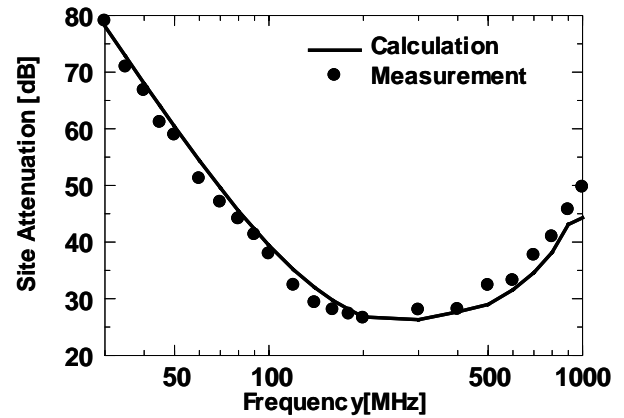
$$F_a (dB) = (S_{ATT} (dB) - N_{ATT} (dB)) / 2 \quad (4)$$

Where, N_{ATT} is normalized site attenuation [9].

Calculation result is shown in Fig. 9. The measurement was carried out in large semi-anechoic chamber, and receiving antenna was placed 2 m high from ground plane. A calibrated half wave dipole antenna was used as reference. This shows that the measurement value is almost agree with the calculating one. This means that the antenna factor of the antenna can be calculated by the model in this paper.



(a) Vertical polarization



(b) Horizontal polarization

Fig. 8 Measurement and calculated result of site attenuation when transmitting antenna height is 1m

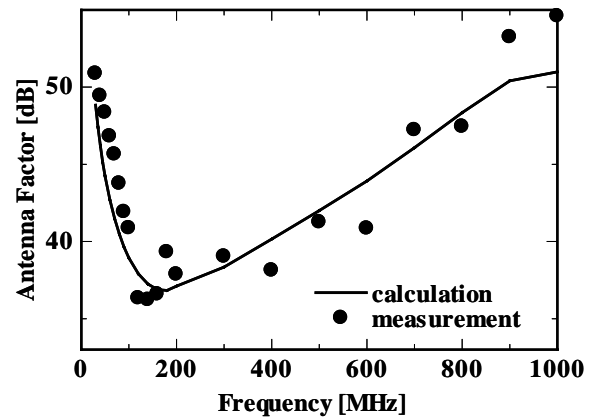


Fig. 9 Antenna Factor of Wire grid Model of Spherical Dipole Antenna

4. EVALUATION OF EMC MEASUREMENT FACILITIES USING SHERICAL DIPOLE ANTENNA

The site attenuation of the spherical dipole antenna is useful to evaluate small semi-anechoic chamber because the antenna size is small compared with dipole antenna and biconical antenna. This section describes evaluation results of the semi-anechoic chamber whose size is 5.2 m wide, 6 m long, and 5 m high.

4.1 Measurement of site attenuation distribution

Measurement of site attenuation distribution is useful to find the best position placing EUT in anechoic chamber. On the measurement, the transmitting and receiving antenna were placed 1 m high from ground plane and the receiving antenna was moved in the chamber at intervals of 0.5 m.

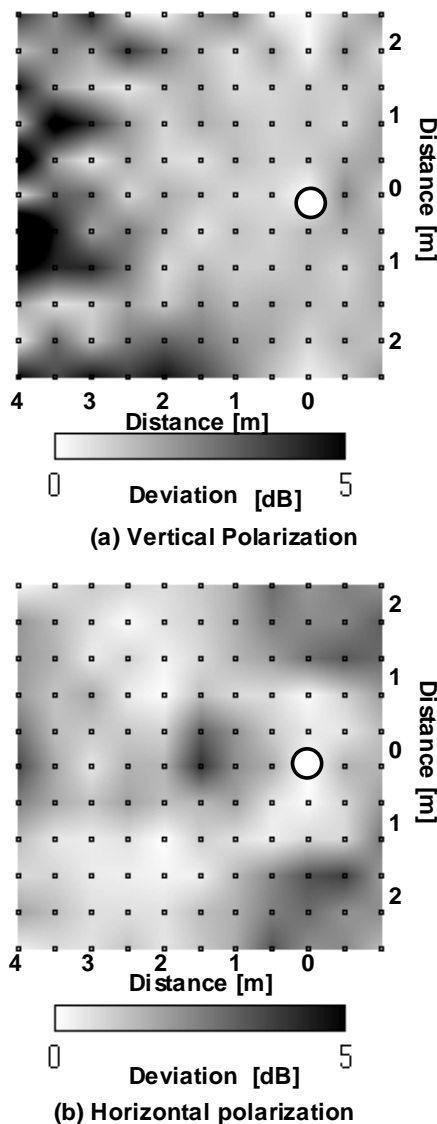


Fig. 10 Site attenuation distribution at 300MHz

The result is shown in Fig. 10. This shows the deviation between measured and calculated value. The circles in these figures indicate the position of transmitting antenna. These indicate that the site attenuation characteristics may be improved when transmitting antenna and receiving antenna are placed line unsymmetrical position.

4.2 Measurement of absorber influence

The semi-anechoic chamber shown in Fig. 11 is used the different types of the radio wave absorbers. Absorber A improves the reflection loss around 200 MHz compared with absorber B. However, absorber A is lined in limited place as shown in Fig. 11, and it can be estimated that the limited installation may reduced the performance of the chamber. The influence of the absorber layout was examined by the site attenuation of the spherical dipole antenna.

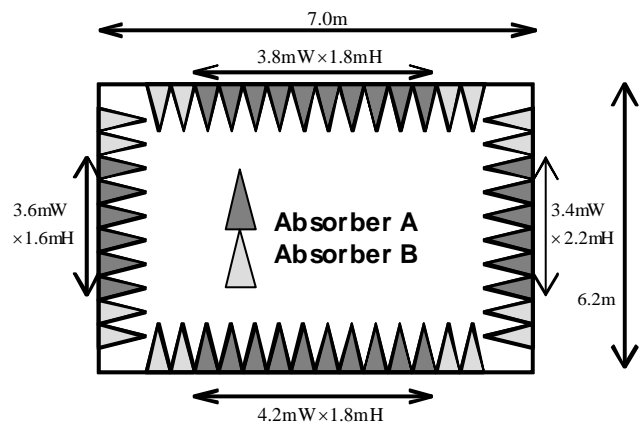


Fig. 11 Layout of absorbers in semi-anechoic chamber

The site attenuation distribution was measured at the height of 3 m, where absorber B used roof and sidewalls. The frequency of 300 MHz was selected because the reflection loss of absorber B is smaller than that of absorber A. For comparison, the frequency of 600 MHz, where the reflection loss of absorber A is almost the same as that of absorber B. Vertical polarization was selected because the influence of side wall was larger than that of horizontal polarization.

Measurement results are shown in Figs. 12 and 13. Figure 12 shows the measurement results of site attenuation distribution at 3 m high. To compare with Fig. 10(a), it is clear that the deviation from calculation value in Fig. 12(a) is larger than that in Fig. 10 (a). These indicate that the low reflection loss absorber reduces the performance at higher area of the chamber.

Figure 13 shows the site attenuation distribution at 600 MHz at 3 m high. These indicate that the deviation from calculation value is smaller than that in Fig. 10(a). Considering with the reflection loss absorber B at 600 MHz is larger than that of absorber A at 300 MHz, this means that

the performance of the chamber might be improved if the absorber B is replaced by absorber A.

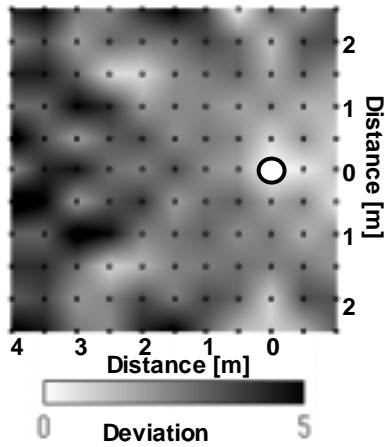


Fig. 12 Site attenuation distribution at 300MHz when antenna height is 3m and polarization is vertical

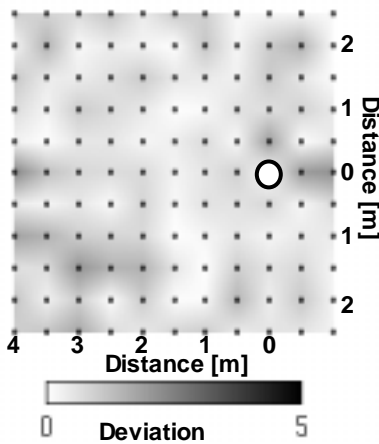


Fig. 13 Site attenuation distribution at 600MHz when antenna height is 3m and polarization is vertical

5. CONCLUSION

Calculation method of site attenuation for spherical dipole antenna was developed using wire grid model. The number of wire and segment were investigated to achieve the solutions whose deviation from measured value could be the minimize. The calculated results were compared with measured one in semi-anechoic chamber. The result indicated the deviation between calculation and measurement result was within 4dB from 30 MHz to 1000MHz. The antenna factor of the spherical dipole antenna was cal-

culated from the site attenuation. The results were almost agreed with the measured one.

The site attenuation of the spherical dipole was applied to evaluate a small semi-anechoic chamber. The results indicated that the site attenuation characteristics were improved when the transmitting and receiving antenna were placed at line unsymmetrical position. It also indicated that the site attenuation might be improved if the absorbers were replaced by the absorber whose reflection loss is larger than that of conventional one.

The future problem is reducing the deviation between measurement and calculation value .

References

- [1] J. C. Matovani and D. N. Herman, "A spherical dipole source for use as a transfer standard between radiated emission test sites", IEEE International Symposium on EMC, pp. 583-588, Tokyo, 1984
- [2] K. Murakawa, N. Kuwabara, and F. Amemiya, " Radiation properties of spherical dipole antenna", IEEE International Symposium on EMC, pp.572-576 Nagoya, 1989
- [3] N. Kuwabara, K. Tajima, R. Kobayashi, and F. Amemiya, "Development and analysis of electric filed sensor using LiNbO₃ optical Modulator", IEEE Trans. Electromagn. Compat., vol. EMC-34. no. 4, pp. 391-395, Nov. 1992
- [4] T. Mori, K. Shinozaki and Y. Kaneko, "Improving shielding effectiveness measurement with spherical dipole antenna", IEEE International Symposium on EMC, pp.1-4, Chicago, 1994
- [5] A. Sugiura, M. Okamura " Correction factors for the normalized site attenuation", IEEE International Symposium on EMC, pp.29-34 Nagoya, 1989
- [6] K. Gyoda, A. Nishikata, T. Shinozuka and A. Sugiura " Analysis of biconical antenna for EMC measurement", IEEE International Symposium on EMC, pp.755-758 Nagoya, 1994
- [7] Roger F. Harrington, "Field Computation by Moment Methods," IEEE Press, 1992
- [8] G. J. Burke and A. J. Poggio, "Numerical Electromagnetics Code (NEC) - Method of Moments, Part I-III, Lawrence Livermore Laboratory, 1981
- [9] A. A. Smith, Jr., "Calculation of site attenuation from antenna factors," IEEE Trans. Electromagn. Compat, vol. EMC-24, no.3, pp.301-316, 1982.